

1 **Assessing Recovery Time of Ecosystems in China: Insights into Flash** 2 **Drought Impacts on Gross Primary Productivity**

3 Mengge Lu^{1,2}, Huaiwei Sun^{1,3,4*}, Yong Yang¹, Jie Xue⁵, Hongbo Ling⁵, Hong Zhang⁶, Wenxin Zhang²

4 ¹School of Civil and Hydraulic Engineering, Huazhong University of Science and Technology, Wuhan 430074, China.

5 ²Department of Physical Geography and Ecosystem Science, Lund University, Sölvegatan 12, 22362 Lund, Sweden.

6 ³College of Water Conservancy & Architectural Engineering, Shihezi University, Shihezi 832000, China.

7 ⁴Hubei Key Laboratory of Digital River Basin Science and Technology, Huazhong University of Science and Technology,
8 Wuhan 430074, China.

9 ⁵State Key Laboratory of Desert and Oasis Ecology, Xinjiang Institute of Ecology and Geography, Chinese Academy of
10 Sciences, Urumqi 830011, China.

11 ⁶School of Engineering and Built Environment, Griffith University, Gold Coast Campus, 4222, QLD, Australia.

12

13 *Correspondence to:* Huaiwei Sun (hsun@hust.edu.cn)

14

15

16 **Abstract.** Recovery time, referring to the duration an ecosystem needs to return to its pre-drought condition, is a fundamental
17 indicator of ecological resilience. Recently, flash droughts (FDs) characterized by rapid onset and development have gained
18 increasing attention. Nevertheless, the spatiotemporal patterns of gross primary productivity (GPP) recovery time and the
19 factors influencing it remain largely unknown. In this study, we investigate the recovery time patterns of terrestrial ecosystem
20 in China based on GPP using a Random Forest (RF) regression model and the Shapley Additive Prediction (SHAP) method.
21 A random forest regression model was developed for analyzing the factors influencing recovery time and establish response
22 functions through partial correlation for typical flash drought recovery periods. The dominant driving factors of recovery time
23 were determined by using the SHAP method. The results reveal that the average recovery time across China is approximately
24 37.5 days, with central and southern regions experiencing the longest durations. Post-flash drought radiation emerges as the
25 primary environmental factor, followed by aridity index and post-flash drought temperature, particularly in semi-arid/sub-
26 humid areas. Temperature exhibits a non-monotonic relationship with recovery time, where both excessively cold and hot
27 conditions lead to longer recovery periods. Herbaceous vegetation recovers more rapidly than woody forests, with deciduous
28 broadleaf forests demonstrating the shortest recovery time. This study provides valuable insights for comprehensive water
29 resource and ecosystem management and contributes to large-scale drought monitoring efforts.

30 **1 Introduction**

31 Climate change has exacerbated drought, which has significant implications for achievement the Sustainable Development
32 Goals (SDGs) (Lindoso et al., 2018). Among the 17 SDGs outlined in the 2030 Agenda, at least five are directly linked to
33 drought: Goal 6 “Clean water and sanitation”, Goal 11 “Sustainable cities and communities”, Goal 12 “Responsible production
34 and consumption”, Goal 13 “Climate action”, and Goal 15 “Life on land” (Zhang et al., 2019; Nilsson et al., 2016). Flash
35 droughts, characterized by rapid onset and intensification, have gained increasing recognition among hydrologist and general

36 public globally (Yuan et al., 2023). These events significantly impact terrestrial ecosystem productivity, photosynthesis, and
37 latent heat fluxes (Zhang et al., 2020a; Yang et al., 2023). The effects of flash droughts are not only felt during the events but
38 also persist in their aftermath, with legacy effects post-drought (Liu et al., 2023a). Recovery time—defined as the duration
39 required for an ecosystem to return to its pre-drought state, is a fundamental aspect of ecological resilience (Schwalm et al.,
40 2017; Wu et al., 2017). Recovery time is related to ecological thresholds, as it may trigger a critical "tipping point" that lead
41 to shifts into new ecosystem state (Lenton et al., 2008). With the expectation of more frequent and severe flash droughts in the
42 future (Sreeparvathy & Srinivas, 2022), exploring post-flash drought recovery trajectories is of paramount importance (Jiao et
43 al., 2021).

44 Drought recovery characteristics have been extensively observed at the ecosystem scale, typically using tree ring records,
45 productivity or greenness measurements, and satellite data (Gazol et al., 2017; Kannenberg et al., 2019). These studies have
46 identified varied recovery times across regions and ecosystems. Grasslands exhibit longer recovery times compared to other
47 land covers types due to shallow-rooted plants and lower soil water retention capacity (Hao et al., 2023). Conversely, recovery
48 in croplands is more influenced by human farming practices (Darnhofer et al., 2016). In forests, mixed forests tend to recover
49 more quickly, whereas deciduous broadleaf forests have the longest recovery periods (He et al., 2018). Hydro-meteorological
50 conditions also play a role, with semi-arid and semi-humid regions experiencing longer recovery times than humid and arid
51 regions (Zhang et al., 2021). The longer recovery time in semi-arid and semi-humid regions may be related to the specific
52 challenges these regions face, such as soil conditions, water availability, and climatic variability (Huxman et al., 2004; Zhang
53 et al., 2021).

54 However, the contribution of driving factors in flash drought recovery remains unclear. Some studies indicate that background
55 value, drought return interval, post-drought meteor-hydrological conditions, and drought attributes (such as duration, intensity)
56 are critical in regulating recovery (Kannenberg et al., 2020). Lower background value may result in more severe damage,
57 abnormal post-drought meteor-hydrological conditions, and longer recovery times (Fu et al., 2017). Greater drought intensity
58 and longer duration can lead to significant ecosystem losses (Godde et al., 2019). Favorable post-drought meteor-hydrological
59 conditions (e.g., increased precipitation and suitable temperature) improve the chance of complete recovery (Jiao et al., 2021).
60 Plant physiological response, including changes in leaf water potential and phenology, also play a crucial role in the recovery
61 process (Miyashita et al., 2005).

62 While the impacts of flash droughts on ecosystems have been well-documented, the recovery process remains underexplored.
63 For instance, studies show that solar-induced fluorescence (SIF) and SIF yield values decline post-flash drought (Yao et al.,
64 2022), and 95% of the gross primary production (GPP) in the Indian region responded to flash droughts with an average
65 response time of 10-19 days (Poonia et al., 2021). However, most research focus on the immediate ecological responses to
66 flash droughts, rather than on the recovery process (Otkin et al., 2019). Notably, a substantial contrast exists in the definition
67 of recovery stages between flash droughts and traditional slow droughts (Wang et al., 2016). These results lead to the

68 conclusion that recovery is a part of the former, while the recovery phase of the latter usually occurs at the end of the event
69 (Qing et al., 2022). Furthermore, some studies suggest that flash drought recovery is more reliant on changes in soil moisture
70 or peak evapotranspiration, while traditional slow drought recovery is typically assessed using ecological or hydrological
71 indicators (Xu et al., 2023). For example, China has experienced frequent flash from 1980 to 2021, particularly in southwestern
72 and central regions (Wang et al., 2022a). Moreover, there may be more severe and frequent flash droughts in the future
73 (Christian et al., 2023). Research on flash drought recovery in Xiang and Wei River Basin found that most events recovered
74 within 28 days (Wang et al., 2023a). However, there remains a lack of comprehensive studies on flash drought recovery and
75 the factors influencing its spatiotemporal patterns across China.

76 Drought can lead to water shortages, limiting access to clean drinking water. Effective drought management is therefore crucial
77 for achieving SDGs. By utilizing newly available datasets and hydro-meteorological variables in China, this study assesses the
78 extent of post-flash drought impacts, documents recovery times, and analyzes the factors contributing to variations in
79 ecosystem recovery. The objectives of this study are to: (1) investigate the spatial pattern of post-flash drought recovery; (2)
80 identify the most critical determinants of recovery; and (3) analyze the impact of various factors on flash drought recovery
81 times. The following sections include Section 2, which provides a brief description of data and methods, Section 3, which
82 presents the results presented by novel methods applied. Then, we provide a detailed discussion in Section 4. Section 5 gives
83 the conclusions with some more information presented in supplementary materials.

84 **2 Data and methods**

85 **2.1 Data**

86 **2.1.1 Soil moisture datasets**

87 Daily root-zone soil moisture (SM) data for the period of 2001-2018 are obtained from Global Land Evaporation Amsterdam
88 Model (GLEAM) (<https://www.gleam.eu/>). GLEAM estimates root-zone soil moisture using a multi-layer water balance
89 approach. The depth of the root zone varies based on the type of land cover. For tall vegetation (e.g. trees), the depth is divided
90 into three layers (0-10 cm, 10-100 cm, and 100-250 cm); For low vegetation (e.g. grass), there are two layers (0-10 cm and
91 10-100 cm); Bare soil only has one layer (0-10 cm) (Martens et al., 2017; Miralles et al., 2011). It has been widely applied in
92 the identification and impact assessment of flash drought events (Zha et al., 2023). We utilized the bilinear interpolation method
93 to resample SM from a spatial resolution of 0.25° to 0.1°, aligning it with the accuracy of other datasets. This method is
94 appropriate for continuous input values, easy to implement, and generally effective in converting coarse input data into spatially
95 refined output (Chen et al., 2020).

96 2.1.2 Hydro-meteorological datasets of affecting variables of recovery time

97 We analyse the recovery time considering multiple influencing factors such as meteorological variables, drought-related
98 variables, and land cover (He et al., 2018). Meteorological data from the China Meteorological Forcing Dataset (CMFD),
99 accessible at <https://westdc.westgis.ac.cn/>, is utilized for the period spanning 2001 to 2018 (Yang et al., 2019). The near-
100 surface air temperature, downward shortwave radiation, downward longwave radiation, precipitation rate and wind speed are
101 used in this study. VPD is calculated based on temperature, and specific humidity using Eq. (1) - (3) (Peixoto & Oort. 1996)
102 (Zotarelli et al., 2020).

$$103 \quad SVP = 0.618 \exp\left(\frac{17.27T}{T+273.73}\right) \quad (1)$$

$$104 \quad AVP \approx \frac{q_s p}{\varepsilon} \quad (2)$$

$$105 \quad VPD = SVP - AVP \quad (3)$$

106 where SVP and AVP is saturated vapor pressure and actual vapor pressure (kPa), respectively. And T is temperatures ($^{\circ}\text{C}$), q_s is
107 the specific humidity, p is the atmospheric pressure (kPa), $\varepsilon = 6.22$ is the ratio of water vapor molecular weight to dry air weight.

108 Aridity index is calculated as the ratio of precipitation to potential evapotranspiration. Typically, the multi-year average of the
109 aridity index serves as an indicator of water availability and drought timing within a particular region (Huang et al., 2016).
110 Aridity index is obtained from <https://doi.org/10.6084/m9.figshare.7504448.v5> (Zomer et al., 2022). To analyze the distinct
111 responses of different vegetation types, we employ the MODIS dataset from the International Geosphere-Biosphere
112 Programme (IGBP) MCD12C1 (Friedl et al., 2002) (Figure. S1).

113 2.1.3 Gross primary productivity

114 Gross Primary Productivity (GPP) is widely used as an indicator for monitoring post drought photosynthesis dynamics (Gazol
115 et al., 2018). The FluxSat GPP dataset (Version 2), derived from Moderate Resolution Imaging Spectroradiometer (MODIS),
116 is calibrated using FLUXNET 2015 and OneFlux tier 1 data, and validated with independent datasets (Joiner et al., 2021).

117 It shows strong agreement with flux data at most sites and performs reliably across a majority of global regions (Bennett et al.,
118 2021). Additionally, it has been widely used in examining the impacts of extreme climate events on the terrestrial carbon cycle
119 (Byrne et al., 2021). The dataset provides a spatial resolution of 0.05° and a daily temporal resolution. To match the flash
120 drought event, daily soil moisture data were resampled to 0.1° and aggregated to pentad-mean (five-days) data. This study
121 chooses the growing seasons (April to October) from 2001 to 2023 as the study period.

122 2.2 Method

123 2.2.1 The identification of flash drought events and recovery time

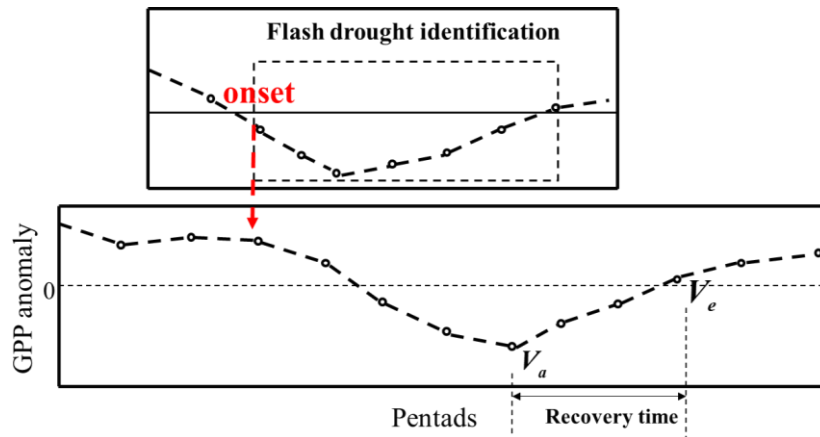
124 In this study, we identify flash drought events by analysing changes in soil moisture, taking into account their rapid
125 intensification and duration. Evaporation demand is often used as a warning indicator for flash droughts (Rigden et al., 2020).

126 Because it may overestimate flash droughts (Lesinger & Tian. 2022). To identify flash drought events, the daily soil moisture
 127 data is aggregated into pentad-mean data. These averages are then converted into percentiles based on the climatology of each
 128 pentad period during the growing season. The identification of flash droughts should meet the following criteria: soil moisture
 129 (SM) must decrease from above the 40th percentile to below the 20th percentile within a 5-day period, with an average rate of
 130 decline per pentad not less than the 5th percentile. A flash drought terminates if the declining SM rises back to the 20th
 131 percentile. The duration of a flash drought event must be at least 4 pentads (20 days) (Yuan et al., 2019, Zhang et al., 2020a).
 132 The speed of flash drought (Ospd) is the ratio of the difference between the 40th percentile and the lowest percentile of the
 133 onset stage to the length of onset. The frequency refers to the overall number of occurrences within a given time frame (e.g.,
 134 per year or per decade). Severity is the accumulated soil moisture percentile deficits from the threshold of 40th. We employed
 135 anomaly GPP to estimate post-flash drought vegetation recovery times at the pixel scale. The recovery time was defined as the
 136 period between the point when GPP reached its maximum loss and when it returned to its pre-flash drought level (Wang et
 137 al., 2023a) (Figure.1). To ensure data consistency and minimize noise, we first applied a smoothing process to the pentad GPP
 138 data using a 3-pentad forward-moving window at the pixel scale. After smoothing the data, we calculate the GPP anomaly
 139 using the following equation:

$$140 \text{ GPP anomaly} = \frac{GPP - \mu_{GPP}}{\sigma_{GPP}} \quad (4)$$

141 where, μ_{GPP} and σ_{GPP} are mean and standard deviation of the pentad time series of GPP.

142 The beginning of the recovery stage is identified when the post-flash drought GPP anomaly is negative and reaches its
 143 minimum value, indicating the point of maximum GPP loss. The recovery stage concludes when the GPP anomaly returns to
 144 a positive value, signifying that productivity has reached or exceeded its pre-drought level. However, if no flash drought event
 145 occurs during the period of negative GPP anomaly, if the GPP anomaly is already negative before the onset of the flash drought
 146 event, or if negative GPP anomalies only occur for one pentad, the corresponding GPP data series is excluded from the analysis
 147 to prevent misleading results.



148

149 **Figure 1. The identification of recovery time.** GPP anomaly is detrended vegetation production index on a time series, 0 is
 150 defined as the threshold of a negative anomaly. Below the dashed line represents that vegetation production is in a negative
 151 abnormal state. We quantify recovery time as: the recovery time begins when the vegetation production loss reaches the
 152 maximum and ends when the detrended vegetation production index is above 0.

153 2.2.2 Response functions

154 Partial dependence plots based on the random forest algorithm are utilized for visualizing response functions (Schwalm et al.,
 155 2017; Sun et al., 2016). The analysis of partial dependence focuses on evaluating the marginal impact of a covariate (or
 156 independent variable) on the response variable, while keeping other covariates constant (Liaw & Wiener, 2002). It facilitates
 157 the exploration of insights within large datasets, particularly when random forests are primarily influenced by low-order
 158 interactions (Martin, 2014). In addition, it is valuable tools for identifying significant features, detecting non-linear
 159 relationships, and gaining insights into the overall behavior of a predictive model.

160 2.2.3 Attribution analysis of ecosystem recovery

161 In order to better understand the potential factors driving terrestrial ecosystem productivity recovery after flash droughts, we
 162 conduct attribution analysis. We selected downward radiation (the sum of downward shortwave radiation and downward
 163 shortwave radiation), temperature, wind speed, precipitation rate, VPD, flash drought speed (Ospd), flash drought severity
 164 (Osev), flash drought duration (Odur), aridity index, land cover types as explanatory variables. It should be noted that these
 165 variables are considered within the recovery period. The feature importance of random forest can only indicate the extent to
 166 which the input variables influence the model's output, but it does not reveal how these input variables specifically impact the
 167 model's output (Wang et al., 2022b). The Shapley Additive Prediction (SHAP) method has emerged as a valuable tool that
 168 addresses the limitations of traditional machine learning methods (Štrumbelj&Kononenko,2014). As a result, the SHAP
 169 method is widely utilized in attribution analysis of variables (Wang et al., 2022b; Lundberg & Lee, 2017).

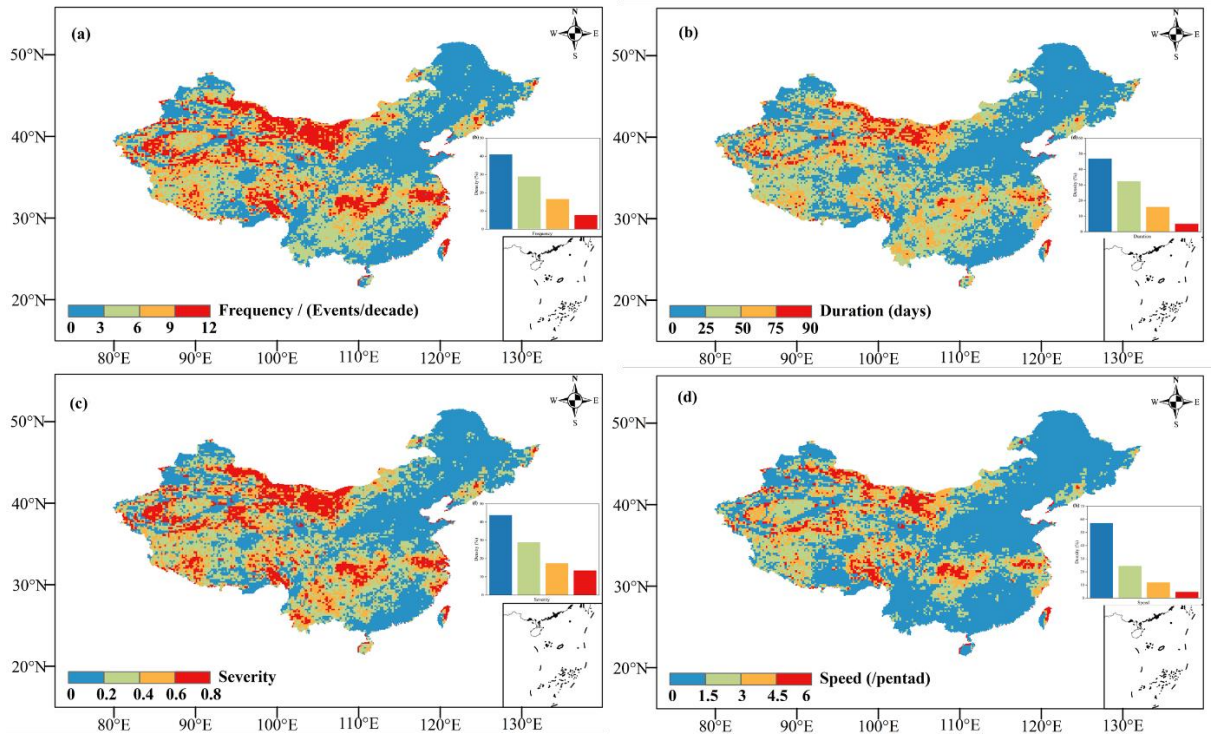
$$170 \quad \varphi_m(v) = \sum_{S \subseteq N \setminus \{m\}} \frac{|S|!(|N|-|S|-1)!}{|N|!} (v(S \cup \{m\}) - v(S)) \quad (5)$$

171 where, $\varphi_m(v)$ represents the contribution of covariate m , N denotes the set of all covariates, S is a subset of N , and $v(S)$
 172 represents the value of that subset.

173 We utilized a random forest model and employed these variables as predictive factors to estimate the productivity recovery
 174 time for all study grid cells. Then, we used the SHAP value to quantify the marginal contribution of each predictive variable
 175 and rank their relative importance based on the average absolute SHAP value.

177 **3.1 Characteristics of flash droughts**

178 Figure 2 presents the frequency, duration, severity, and speed of flash droughts over China during 2001-2019. Approximately
 179 7% of grids did not experience a flash drought event, while the remaining 93% of grids experienced at least one event. The
 180 middle and lower reaches of the Yangtze River exhibited a high frequency value with above 12 events/decade, whereas other
 181 regions mainly ranged from 0 to 9 events/decade. There is a clear spatial pattern for the duration, ranging from 0 to 20 days
 182 over China. The Southwestern and the middle and lower reaches of the Yangtze River had longer durations, exceeding 90 days
 183 (Figure. S2). In addition to the higher severity of flash droughts in the southwest region, a similar spatial pattern was observed
 184 for severity and speed. Regarding speed, areas with faster speed were primarily concentrated in the lower reaches of the
 185 Yangtze River. Overall, the middle and lower reaches of the Yangtze River and the southwestern region are considered hot
 186 spots, although the latter's speed is not rapid.

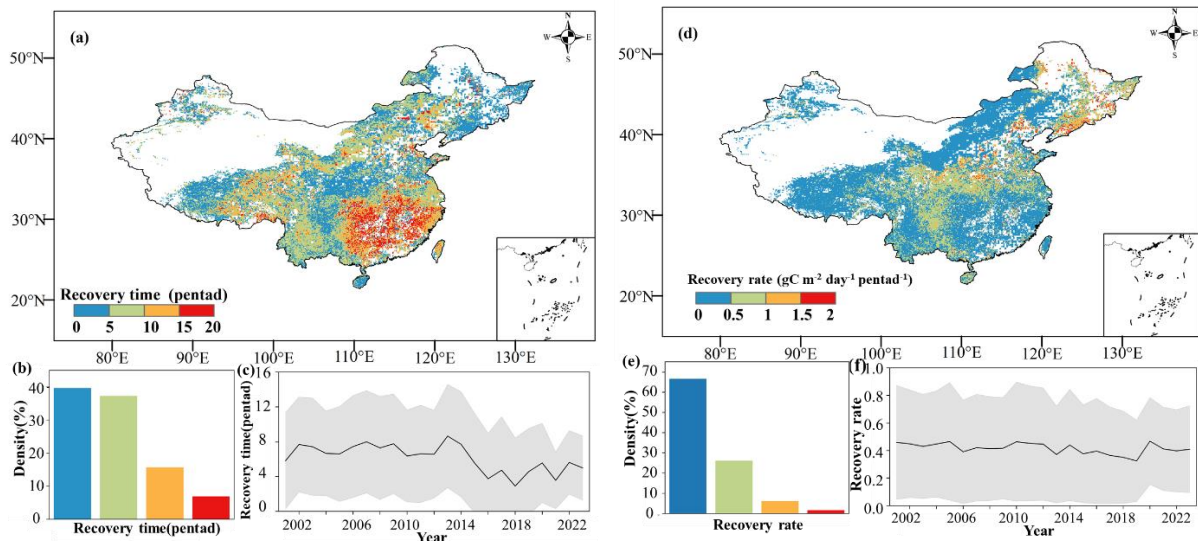


187
 188 **Figure 2. Frequency (a), duration (b), severity (c), speed (d) of flash drought over China during 2001–2023.**

189 **3.2 Spatial pattern of ecosystem recovery time and recovery rate**

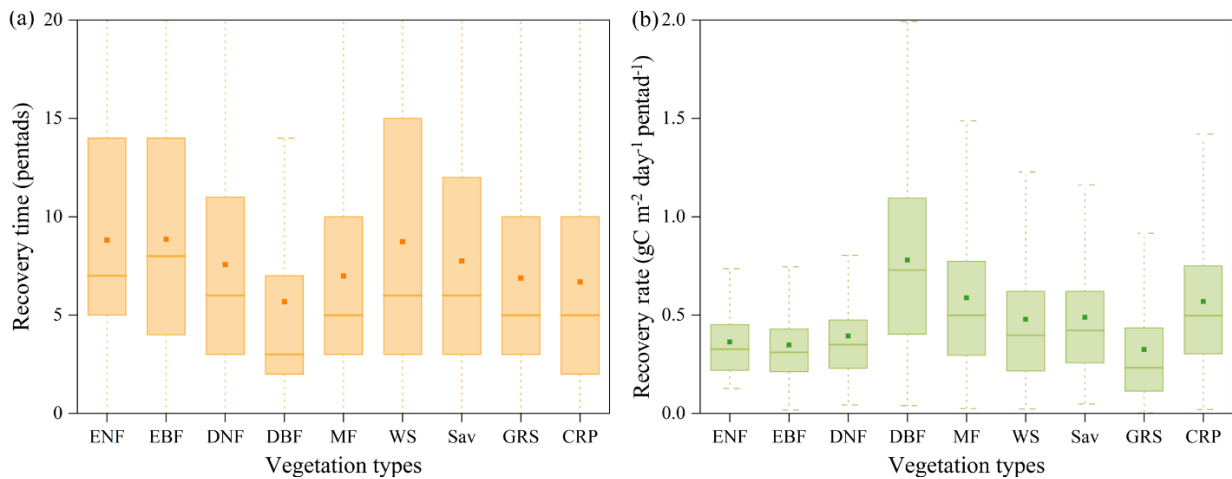
190 Vegetation productivity showed a clear response to flash droughts, and this response typically had a certain lag (Figure. S3).
 191 Ecosystems exhibited distinct spatial differences in recovery times to flash droughts (Figure. 3). The mean recovery time for

192 Chinese ecosystems was 37.5 days (7.5 pentads) calculated by GPP. Most regions were able to recover to their normal state
 193 within 50 days. However, certain areas, such as central China and southern China, required 90 days or more to recover. In
 194 terms of time series, there was no evident trend in the mean recovery time, with fluctuations occurring within 7.5 pentads. On
 195 average, the recovery rate of grids in China ranged from 0 to 2 per pentad, and approximately 90% of grids had a recovery rate
 196 of less than 1 per pentad. There is no significant trend in recovery rate over time. To further illustrate the impact and recovery
 197 of flash droughts on different vegetation types, we calculated the recovery time and recovery rate for each type (Figure. 4).
 198 Among the different vegetation types, DBF had a shorter recovery time and a higher recovery rate. Additionally, CRP showed
 199 moderate recovery rates, while GRS had relatively low rates of recovery. This reflects the fact that flash droughts had a more
 200 significant impact on GRS and resulted in greater productivity losses. By employing various recovery thresholds (80%, 90%,
 201 100%, and 110% of the original state), we confirmed although the recovery time of some grid pixels can vary, the overall
 202 spatial pattern of recovery time remains consistent regardless of the threshold (Figure.S4).



203

204 **Figure 3. Spatial pattern of recovery time (a-c) and recovery rate (d-f).** (a) and (d) represent the recovery time (pentad)
 205 and recovery rate ($\text{gC m}^{-2} \text{day}^{-1} \text{pentad}^{-1}$) calculated by using GPP data respectively. (b) and (e) represent the density of different
 206 recovery times and recovery rate respectively, the horizontal axis represents the recovery time (pentad), recovery rate (gC m^{-2}
 207 $\text{day}^{-1} \text{pentad}^{-1}$) and the vertical axis is the density. Regions with sparse GPP or no droughts are masked with white.

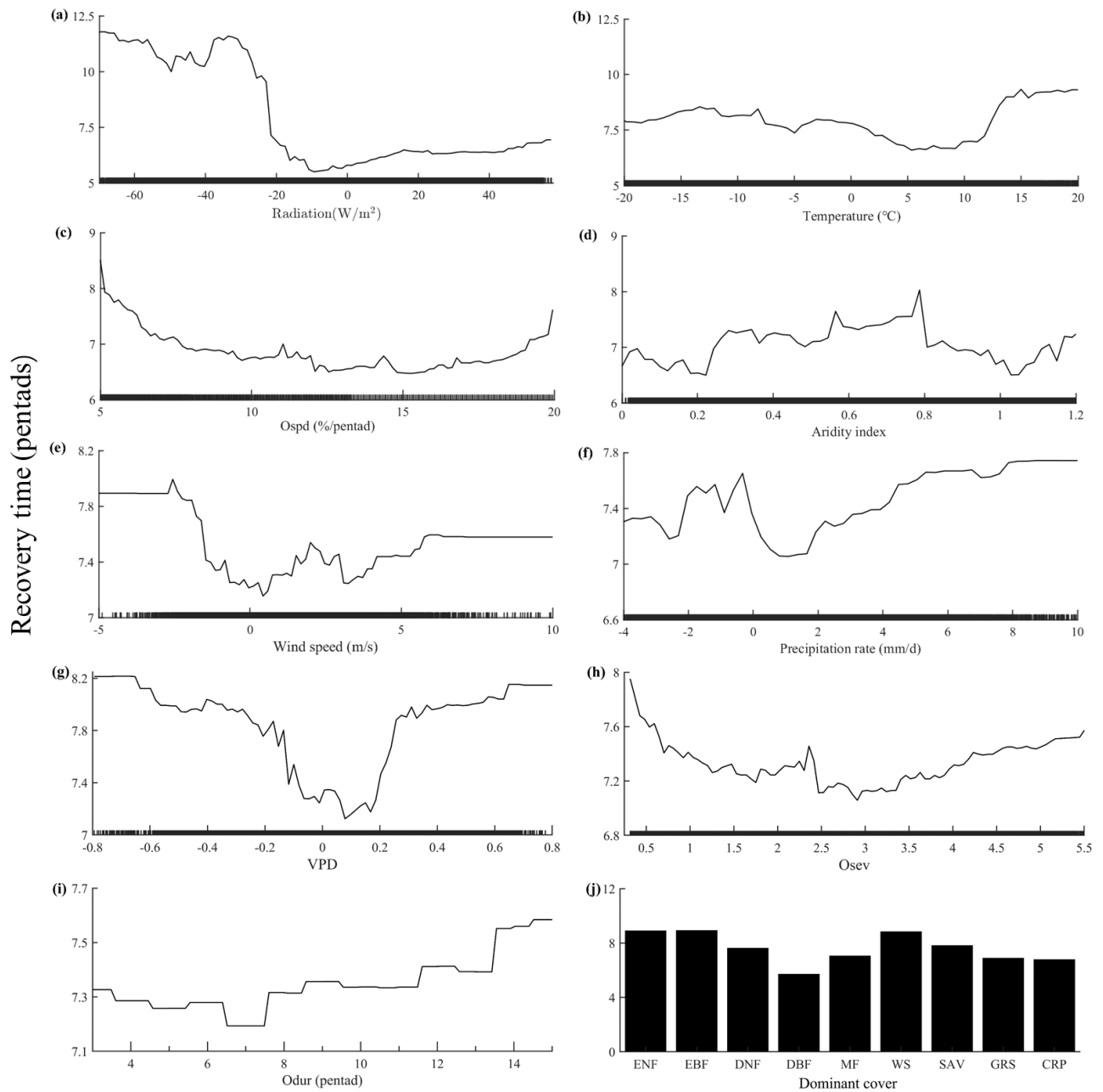


208

209 **Figure 4. The recovery time and recovery rate across different vegetation types.** The vegetation types are: ENF (evergreen
 210 coniferous forest), EBF (evergreen broad-leaved forest), DNF (deciduous coniferous forest), DBF (deciduous broad-leaved
 211 forest), MF (mixed forests), WS (closed shrubland, open shrubland, and woody savannas), SAV (savannas (temperate)), GRS
 212 (grasslands), CRP (croplands).

213 3.3 Response functions for flash drought recovery time

214 The random forest regression model explained 55% of the out-of-bag variance in recovery time (Figure. 5). Radiation emerged
 215 as the most influential factor impacting flash drought recovery time, with lower solar radiation conditions leading to prolonged
 216 the recovery time (Figure. 5a). Temperature did not exhibit a monotonic response in relation to recovery time. Excessively
 217 cold or overheated temperatures resulted in longer recovery times, whereas slightly higher temperatures promoted vegetation
 218 recovery (Figure. 5b). Specifically, a slight increase in temperature facilitated vegetation restoration, while higher temperatures
 219 extended the recovery time of flash droughts. This suggests that the projected rise in extreme high temperatures will further
 220 lengthen the recovery time (Li et al., 2019). In terms of flash drought characteristics, the difference in recovery time was
 221 related to the discrepancy in severity and duration, albeit to a lesser extent than speed (Figure. 5c, h & i). Recovery time
 222 increased in a stepwise manner as the duration increased. Ecosystems experiencing prolonged durations of flash droughts
 223 typically exhibit longer recovery times. In addition, semi-arid/sub-humid areas ($0.2 < AI < 0.65$) have longer recovery times
 224 (Figure. 5d). The wind speed exhibited a bimodal pattern, indicating that the recovery time was shortest when it closely aligned
 225 with the multi-year average or was 3.5 times higher than the multi-year average (Fig. 5e). Adequate precipitation following a
 226 flash drought assisted in recovery, although excessively extreme precipitation could also hinder it (Fig. 5f). Extreme vapor
 227 pressure deficit (VPD), whether high or low, prolonged the recovery time (Fig. 5g). Among different vegetation types,
 228 herbaceous vegetation recovered more rapidly than woody forests. Deciduous broadleaf forests (DBF) demonstrated the
 229 shortest recovery time (Figure. 5j).

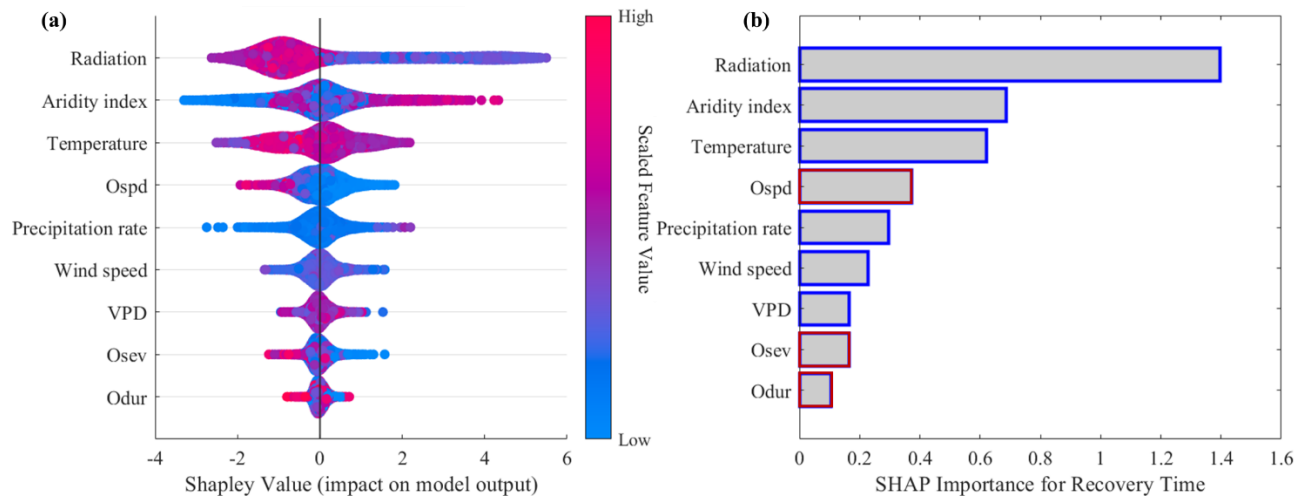


230

231 **Figure 5. Response functions for flash drought recovery time**, reflecting the response of recovery time to a single dependent
 232 variable when others are unchanged. Note difference in the y-axis scales. The covariates a to j are the deviations from the
 233 baseline. Positive (negative) indicates above (below) the average value.

234 3.4 Drivers of flash drought recovery time

235 We then performed an attribution analysis using SHAP method to quantify the relative importance of the considered variables.
236 The results were consistent with the results of section 3.3. In general, radiation and aridity index were the most relevant controls
237 of spatial variations of post-flash drought recovery time (Figure 6). Temperature was the third most impactful variable overall,
238 primarily due to its high impact in predicting the recovery time where it has an absolute mean SHAP value of 0.62. Compared
239 to other variables, the impact of speed and duration of flash droughts were relatively low. In addition, during the process of
240 flash drought recovery, the losses caused by flash droughts can also affect productivity recovery. The relationship between
241 recovery time and the attributes of flash drought (speed, severity, duration) is usually negative. That is to say, faster, more
242 severe, and longer lasting flash droughts often have a longer recovery time. Specifically, the speed of flash droughts
243 characteristics is one of the main controlling factors for recovery time.



244 **Figure 6. Identifying drivers of patterns of post-flash drought recovery time.** (a) The summary plot of SHAP values in
245 random forest machine learning. (b) The SHAP Importance (averaged absolute SHAP values) for recovery time. Considered
246 drivers include flash drought characteristics (in red), post-flash drought hydro-meteorological conditions (in blue).
247

248 4 Discussions

249 4.1 Assess flash drought recovery time based on vegetation productivity

250 Given the prevalence of drought in regions over the past few decades, drought is a major natural disaster worldwide (WMO.
251 2021). In addition, its exposure, vulnerability, and risk are expected to further increase under future climate and socio-economic
252 changes (Tabari & Willems. 2018; Cook et al., 2020). Flash drought is widely recognized as a sub-seasonal phenomenon that
253 develops rapidly (Tyagi et al., 2022). Flash droughts have varying degrees of impact on the photosynthesis, productivity, and
254 respiration of ecosystems (Mohammadi et al., 2022). Reducing drought risks and strengthening social drought resistance are

255 also important tasks in order to achieve SDGs by 2030 (Tabari et al., 2023). Flash droughts interact with ecological droughts,
256 with ecological droughts potentially making ecosystems more vulnerable to flash droughts, while flash droughts can exacerbate
257 the effects of persistent ecological droughts (Cravens et al., 2021; Xi et al., 2024). The interplay between these two types of
258 droughts can intensify the pressure on ecosystems, complicating and prolonging the recovery process. The response frequency
259 of Solar-Induced Fluorescence (SIF) in the China basin to flash droughts exceeds 80%, with 96.85% of the regional response
260 occurring within 16 days (Yang et al., 2023). Previous studies have calculated the recovery time of flash drought based on
261 changes in soil moisture, ranging from 8 to 40 days (Otkin et al., 2019). Additionally, the recovery time is generally longer in
262 humid areas compared to arid areas. However, not all flash drought events result in a decrease in ecosystem productivity (Liu
263 et al., 2019). For instance, a study conducted by Zhang et al. (2020b) revealed that between 2003 and 2018, 81% of flash
264 droughts in China displayed negative normalized anomalies in GPP, while the remaining 19% of the events did not exhibit
265 such negative anomalies. Therefore, GPP serves as a more appropriate indicator for monitoring post-drought photosynthesis-
266 related dynamics and evaluating ecosystem recovery time (Yu et al., 2017). Based on GPP, most flash drought events in the
267 Xiangjiang River Basin (XRB) and Weihe River Basin (WRB) recovered within 2 to 8 days. Moreover, the recovery time in
268 the XRB, which is located in a humid area, tends to be longer (Wang et al., 2023a). It should be noted that this study only
269 investigated the aforementioned two watersheds and did not include semi-humid/semi-arid areas. Our study revealed that the
270 average recovery time for flash droughts in the China is approximately 37.5 days (7.5 pentads) (Figure 3).

271 **4.2 The factors that affect drought recovery time**

272 The solar radiation and aridity index were the primary factors that influence the recovery time (Figures 5 & 6, Figure S5). The
273 recovery time was regulated by a combination of drought characteristics (drought return interval, severity, duration), post-
274 drought hydro-meteorological conditions, and vegetation physiological characteristics (Fathi-Taperasht et al., 2022; Liu et al.,
275 2019). Physiological responses, such as the decline rate of productivity upon exposure to flash drought also influence recovery
276 time. Notably, there is a significant negative correlation between the decline rate and the recovery rate (Lu et al., 2024). In the
277 case of flash droughts characterized by rapid development, the speed is one of the most important factors controlling the
278 recovery time (Figure 6). The Yangtze River Basin experienced one of the most severe flash droughts on record during the
279 summer of 2022, primarily driven by abnormal high temperatures and abrupt changes in precipitation (Liu et al., 2023b). The
280 high temperatures accelerated the onset of the drought (Wang et al., 2023b). As a result, the total Gross Primary Production
281 (GPP) loss from July to October 2022 was 26.12 ± 16.09 Tg C, representing a decrease of approximately 6.08% compared to
282 the 2001-2021 average (Li et al., 2024). Ecological drought, characterized by prolonged conditions lasting months to years
283 and resulting in long-term changes to ecosystem functions and structure (Sadiqi et al., 2022). In contrast, flash drought develops
284 rapidly within days to weeks due to extreme weather, leading to immediate reductions in soil moisture and plant health (Yuan
285 et al., 2023). The long-term nature of ecological drought can cause profound impacts such as reduced plant populations,
286 increased soil erosion, and decreased biodiversity, necessitating a longer recovery period (Cravens et al., 2021). In contrast,
287 flash droughts, while shorter in duration, cause rapid plant wilting, reduced crop yields, and soil cracking, with significant

288 long-term consequences for ecosystem recovery (Xi et al., 2024). These two types of droughts can interact, with ecological
289 droughts potentially making ecosystems more susceptible to flash droughts, and flash droughts exacerbating the impacts of
290 ongoing ecological droughts (Hacke et al., 2001; Schwalm et al., 2017). The combined effects of both types can intensify stress
291 on ecosystems, complicating and prolonging the recovery process. Previous studies have shown that the spatial patterns of
292 flash drought recovery were similar to those of precipitation, temperature, and radiation (Wang et al., 2023a). Increased
293 radiation energy and precipitation post a drought can promote vegetation photosynthesis (Zhang et al., 2021). Additionally,
294 there are regional variations in the time required for drought recovery. Generally, semi-arid and semi-humid areas took longer
295 to recover to their pre-drought state (Figure 5). Ecosystems in these areas exhibited higher overall sensitivity to drought
296 (Vicente et al., 2013; Yang et al., 2016). Vegetation in arid areas adapted to long-term water deficit through various
297 physiological, anatomical, and functional mechanisms, resulting in high drought resistance (Craine et al., 2013). In humid
298 areas, sufficient water storage helped resist drought (Liu et al., 2018; Sun et al., 2023). Vegetation also played a crucial role in
299 regulating the recovery trajectory. The drought resistance of plants was determined by various traits such as stomatal
300 conductance, hydraulic conductivity, and cell turgor pressure (Bartlett et al., 2016; Martínez-Vilalta et al., 2017). Grasslands
301 and shrublands could quickly recover from drought, while forest systems require longer periods of time (Gessler et al., 2017).
302 This may be because those have relatively simple vegetation structures, shorter life cycles, and faster growth rates (Ru et al.,
303 2023). In contrast, forest systems have more complex vegetation structures and ecological processes (Tuinenburg et al., 2022).
304 Deep roots enhance tree tolerance to drought (McDowell et al., 2008; Nardini et al., 2016). Compared to shallow roots, deep
305 roots have larger conduit diameters and vessel cells, resulting in higher hydraulic conductivity. During droughts, deep roots
306 may play a critical role in water absorption, as increased root growth with soil depth could represent an adaptation to drought
307 conditions (Germon et al., 2020), enabling rapid access to substantial water reserves stored in deeper soils (Christina et al.,
308 2017).

309 **4.3 Limitations and perspectives**

310 We emphasized that the post-flash drought recovery trajectory of ecosystem is influenced by several factors, including post-
311 flash drought hydrological conditions, flash drought characteristics, and the physiological characteristics of vegetation.
312 However, we should note that in this study, the same percentile threshold (20%, 40%) was used to identify flash drought events
313 based on empirical values from previous research findings. Further investigation should investigate how to determine region-
314 specific thresholds and examine the sensitivity of these thresholds to flash drought recognition (Gou et al., 2022). Furthermore,
315 it is important to consider that plant strategies for coping with flash drought can vary due to species differences (Gupta et al.,
316 2020). There is still a need for improvement in understanding the physiological and ecological mechanisms involved in flash
317 drought recovery. To gain a more comprehensive understanding, future research should explore the mechanism of ecosystem
318 restoration from multiple perspectives, such as evaluating greenness and photosynthesis. Although flash droughts can lead to
319 significant short-term disruptions, there remains a need to explore their long-term effects more comprehensively. Future
320 research should prioritize understanding how these intense, short-term drought events might evolve into more conventional

321 droughts and the persistence of their impacts over time (Liu et al., 2023a). Understanding these dynamics will be crucial for
322 predicting and managing the carbon balance and resilience of ecosystems under changing climate conditions.

323 **5 Conclusions**

324 Effectively reducing drought risk and reducing drought exposure are crucial for achieving sustainable development goals
325 (SDGs) related to health and food security. This study applied a random forest regression model to analyze the factors
326 influencing recovery time and the response functions settled up by partial correlation for typical flash drought recovery time.
327 The most important environmental factor affecting recovery time is post-flash drought radiation, followed by aridity index and
328 post-flash drought temperature. Recovery time prolongs with lower solar radiation conditions. Semi-arid/sub-humid areas have
329 longer recovery time. Temperature does not exhibit a monotonic response in relation to recovery time; excessively cold or
330 overheated temperatures lead to longer recovery times. Herbaceous vegetation recovers more rapidly than woody forests, with
331 deciduous broadleaf forests demonstrating the shortest recovery time.

332 Our study assessed the recovery time of ecosystems to flash droughts based on GPP dataset and identified the dominant factors
333 of recovery time. Results show that 78% of ecosystems could recover within 0 to 50 days. However, certain areas, such as
334 central China and southern China, required 90 days or more to recover. The analysis of the response functions showed that
335 radiation emerged as the most influential factor impacting flash drought recovery time, with lower solar radiation conditions
336 leading to prolonged recovery time. Additionally, temperature did not exhibit a monotonic response in relation to recovery
337 time. In terms of flash drought characteristics, the difference in recovery time is more associated with speed than severity and
338 duration.

339 Although this study provides a good basis for further investigation of flash drought characteristics, it is important to note that
340 the further extension of this study may lead to more understanding of flash drought for hydrological application or worldwide
341 practices. It is important to determine region-specific thresholds and examine the sensitivity of these thresholds to flash drought
342 recognition. Furthermore, plant strategies for coping with flash drought can vary due to species differences. To gain a more
343 comprehensive understanding of flash drought recovery, future research should also explore the mechanism of ecosystem
344 restoration from multiple perspectives, such as evaluating greenness and photosynthesis.

345

346 **Author contributions**

347 **Mengge Lu:** Conceptualization, Methodology, Data curation, Formal analysis, Writing - original draft. **Huaiwei Sun:**
348 Conceptualization, Project administration, Writing - review & editing, Supervision. **Yong Yang:** Writing - review & editing.

349 **Jie Xue:** Writing - review & editing. **Hongbo Lin:** Writing - review & editing. **HongZhang:** Writing - review & editing.
350 **Wenxin Zhang:** Writing - review & editing.

351 **Declaration of competing interest**

352 The authors declare that they have no known competing financial interests or personal relationships that could have appeared
353 to influence the work reported in this paper.

354 **Data availability**

355 Global Land Evaporation Amsterdam Model (GLEAM) soil moisture data is available from <https://www.gleam.eu/>. The China
356 Meteorological Forcing Dataset (CMFD) can be accessed via <https://westdc.westgis.ac.cn/zh-hans/data/7a35329c-c53f-4267-aa07-e0037d913a21/>. The FluxSat GPP dataset (Version 2) dataset is available from <https://daac.ornl.gov>. The MODIS land
357 cover dataset MCD12C1 is available from <https://doi.org/10.24381/cds.f17050d7>.
358

359 **Acknowledgements**

360 This study was funded by the Third Xinjiang Scientific Expedition Program (Grant No.2022xjkk0105) (H.S.). The authors
361 also acknowledge funding from NSFC projects (51879110,52079055, 52011530128). In addition, H.S. acknowledges funding
362 from a NSFC-STINT project (No. 202100-3211). Mengge Lu acknowledges China Scholarship Council (grant number:
363 202306160083).

364 **References**

365 Bartlett, M. K., Klein, T., Jansen, S., Choat, B., & Sack, L., 2016. The correlations and sequence of plant stomatal, hydraulic,
366 and wilting responses to drought. *Proceedings of the National Academy of Sciences of the United States of America*. 113(46),
367 13098-13103.

368 Bennett, B.F., Joiner, J., & Yoshida, Y., 2021. Validating satellite based FluxSat v2. 0 Gross Primary Production (GPP) trends
369 with FluxNet 2015 eddy covariance observations. In, AGU Fall Meeting 2021: AGU.

370 Byrne, B., Liu, J., Lee, M., et al., 2021. The carbon cycle of southeast Australia during 2019–2020: Drought, fires, and
371 subsequent recovery. *AGU Advances*, 2(4), e2021AV000469.

372 Chen, S. L., Xiong, L. H., Ma Q, et al., 2020. Improving daily spatial precipitation estimates by merging gauge observation
373 with multiple satellite-based precipitation products based on the geographically weighted ridge regression method. *Journal of*
374 *Hydrology*. 589: 125156.

375 Christina, M., Nouvellon, Y., Laclau, J. P., et al., 2017. Importance of deep water uptake in tropical eucalypt forest. *Functional*
376 *Ecology*, 31(2), 509-519.

377 Christian, J.I., Martin, E.R., Basara, J.B., et al., 2023. Global projections of flash drought show increased risk in a warming
378 climate. *Commun Earth Environ*. 4, 165.

379 Craine, J. M., Ocheltree, T. W., Nippert, J. B., et al., 2013. Global diversity of drought tolerance and grassland climate-change
380 resilience. *Nature Climate Change*, 3(1), 63–67.

381 Cravens, A. E., McEvoy, J., Zoanni, D., Crausbay, S., Ramirez, A., & Cooper, A. E. 2021. Integrating ecological impacts:
382 perspectives on drought in the Upper Missouri Headwaters, Montana, United States. *Weather, Climate, and Society*, 13(2),
383 363-376.

384 Cook, B. I. et al., 2020. Twenty-first century drought projections in the CMIP6 forcing scenarios. *Earths Future* 8,
385 e2019EF001461.

386 Darnhofer. I., Lamine. C., Strauss. A., et al., 2016. The resilience of family farms: Towards a relational approach. *Journal of*
387 *Rural Studies*. 44: 111-122.

388 Fathi-Taperasht A, Shafizadeh-Moghadam H, Minaei M, et al., 2022. Influence of drought duration and severity on drought
389 recovery period for different land cover types: evaluation using MODIS-based indices. *Ecological Indicators*. 141: 109146.

390 Friedl, M. A., McIver, D. K., Hodges, J. C. F., et al., 2002. Global land cover mapping from MODIS: Algorithms and early
391 results. *Remote Sensing of Environment*. 83(1), 287-302.

392 Fu, Z., Li, D., Hararuk. O., et al., 2017. Recovery time and state change of terrestrial carbon cycle after disturbance.
393 *Environmental Research Letters*. 12(10): 104004.

394 Gazol, A., Camarero, J. J., Anderegg, W. R. L., & Vicente-Serrano, S. M., 2017. Impacts of droughts on the growth resilience
395 of northern hemisphere forests. *Global Ecology and Biogeography*. 26(2), 166–176.

396 Gazol, A., Camarero, J. J., Vicente-Serrano, S. M., et al., 2018. Forest resilience to drought varies across biomes. *Global*
397 *Change Biology*. 24(5), 2143–2158.

398 Gessler, A., Schaub, M., McDowell, N. G., 2017. The role of nutrients in drought-induced tree mortality and recovery. *New*
399 *Phytologist*. 214(2): 513-520.

400 Germon, A., Laclau, J. P., Robin, A., & Jourdan, C. 2020. Tamm Review: Deep fine roots in forest ecosystems: Why dig
401 deeper? *Forest Ecology and Management*, 466, 118135.

402 Godde, C., Dizyee, K., Ash, A., et al., 2019. Climate change and variability impacts on grazing herds: Insights from a system
403 dynamics approach for semi-arid Australian rangelands. *Global change biology*. 25(9): 3091-3109.

404 Gou, Q., Zhu, Y., Lü, H., et al., 2022. Application of an improved spatio-temporal identification method of flash droughts.
405 *Journal of Hydrology*. 604: 127224.

406 Gupta, A., Rico-Medina, A., Caño-Delgado, A I., 2020. The physiology of plant responses to drought. *Science*. 368(6488):
407 266-269.

408 Hacke, U. G., Stiller, V., Sperry, J. S., Pittermann, J. & McCulloh, K. A., 2001. Cavitation fatigue. Embolism and refilling
409 cycles can weaken the cavitation resistance of xylem. *Plant Physiol*. 125, 779-786.

410 Hao, Y., Choi, M., 2023. Recovery of Ecosystem Carbon and Water Fluxes after Drought in China. *Journal of Hydrology*.
411 129766.

412 He, B., Liu, J., Guo, L., et al., 2018. Recovery of ecosystem carbon and energy fluxes from the 2003 drought in Europe and
413 the 2012 drought in the United States. *Geophysical Research Letters*. 45, 4879-4888.

414 Huang, J., Yu, H., Guan, X., Wang, G., & Guo, R., 2016. Accelerated dryland expansion under climate change. *Nature Climate*
415 *Change*, 6(2), 166–171.

416 Huxman, T. E., Smith, M. D., Fay, P. A., et al., 2004. Convergence across biomes to a common rain-use efficiency. *Nature*,
417 429(6992), 651-654.

418 Jiao, T., Williams, C. A., De Kauwe, M. G., et al., 2021. Patterns of post-drought recovery are strongly influenced by drought
419 duration, frequency, post-drought wetness, and bioclimatic setting. *Global Change Biology*, 27, 4630–4643.

420 Joiner, J., and Y. Yoshida. 2021. Global MODIS and FLUXNET-derived Daily Gross Primary Production, V2. ORNL DAAC,
421 Oak Ridge, Tennessee, USA. <https://doi.org/10.3334/ORNLDAAC/1835>.

422 Kannenberg, S. A., Novick, K. A., Alexander, M. R., et al., 2019. Linking drought legacy effects across scales: From leaves
423 to tree rings to ecosystems. *Global Change Biology*, 25(9), 2978–2992.

424 Kannenberg, S. A., Schwalm, C. R., & Anderegg, W. R. L., 2020. Ghosts of the past: How drought legacy effects shape forest
425 functioning and carbon cycling. *Ecology Letters*. 23(5), 891–901.

426 Lenton, T. M., Held, H., Kriegler, E., et al., 2008. Tipping elements in the Earth's climate system. *Proceedings of the national
427 Academy of Sciences*. 105(6), 1786-1793.

428 Lesinger, K., & Tian, D., 2022. Trends, variability, and drivers of flash droughts in the contiguous United States. *Water
429 Resources Research*, 58, e2022WR032186.

430 Lindoso D P, Eiró F, Bursztyn M, et al., 2018. Harvesting water for living with drought: Insights from the Brazilian human
431 coexistence with semi-aridity approach towards achieving the sustainable development goals. *Sustainability*, 10(3): 622.

432 Li, L., Yao, N., Li, Y., et al., 2019. Future projections of extreme temperature events in different sub-regions of China.
433 *Atmospheric research*, 2019, 217: 150-164.

434 Li, T., Wang, S., Chen, B., et al., 2024. Widespread reduction in gross primary productivity caused by the compound heat and
435 drought in Yangtze River Basin in 2022. *Environmental Research Letters*, 19(3), 034048.

436 Liaw, A. & Wiener, M., 2002. Classification and regression by random forest. *R News* 2, 18-22.

437 Liu L, Gudmundsson L, Hauser M, et al., 2019. Revisiting assessments of ecosystem drought recovery. *Environmental
438 Research Letters*. 14(11): 114028.

439 Liu, Y., van Dijk, A. I. J. M., Miralles, et al. 2018. Enhanced canopy growth precedes senescence in 2005 and 2010 Amazonian
440 droughts. *Remote Sensing of Environment*. 211, 26–37.

441 Liu, Y., Zhu, Y., Ren, L., et al., 2023a. Flash drought fades away under the effect of accumulated water deficits: the persistence
442 and transition to conventional drought. *Environmental Research Letters*. 18(11): 114035.

- 443 Liu, Y., Yuan, S., Zhu, Y., et al., 2023b. The patterns, magnitude, and drivers of unprecedented 2022 mega-drought in the
444 Yangtze River Basin, China. *Environmental Research Letters*, 18(11), 114006.
- 445 Lu, M., Sun, H., Cheng, L., et al. 2024. Heterogeneity in vegetation recovery rates post-flash droughts across different
446 ecosystems. *Environmental Research Letters*.
- 447 Lundberg, S. M., & Lee, S. I., 2017. A unified approach to interpreting model predictions. *Advances in neural information*
448 *processing systems*, 30.
- 449 Martin, D. P., 2014. Partial dependence plots. <http://dpmartin42.github.io/posts/r/partial-dependence>.
- 450 Martínez-Vilalta, J., & Garcia-Forner, N., 2017. Water potential regulation, stomatal behaviour and hydraulic transport under
451 drought: Deconstructing the iso/anisohydric concept. *Plant, Cell and Environment*. 40(6), 962–976.
- 452 McDowell, N., Pockman, W. T., Allen, C. D., et al., 2008. Mechanisms of plant survival and mortality during drought: why
453 do some plants survive while others succumb to drought? *New phytologist*, 178(4), 719-739.
- 454 Miyashita, K., Tanakamaru, S., Maitani, T., & Kimura, K., 2005. Recovery responses of photosynthesis, transpiration, and
455 stomatal conductance in kidney bean following drought stress. *Environmental and Experimental Botany*. 53(2), 205–214.
- 456 Mohammadi, K., Jiang, Y., Wang, G., 2022. Flash drought early warning based on the trajectory of solar-induced chlorophyll
457 fluorescence. *Proceedings of the National Academy of Sciences*. 119(32): e2202767119.
- 458 Nardini, A., Casolo, V., Dal Borgo, et al., 2016. Rooting depth, water relations and non-structural carbohydrate dynamics in
459 three woody angiosperms differentially affected by an extreme summer drought. *Plant, Cell & Environment*, 39(3), 618-627.
- 460 Nilsson, M., Griggs, D. & Visbeck, M., 2016. Policy: Map the interactions between Sustainable Development Goals. *Nature*
461 534, 320–322.
- 462 Otkin, J. A., Zhong, Y., Hunt, E. D., et al., 2019. Assessing the evolution of soil moisture and vegetation conditions during a
463 flash drought-flash recovery sequence over the South-Central United States. *Journal of Hydrometeorology*. 20(3): 549-562.
- 464 Peixoto, J. P. and Oort, A. H. 1996. The climatology of relative humidity in the atmosphere, *Journal of Climate*, 9, 3443-3463.
- 465 Poonia, V., Goyal, M. K., Jha, S., et al., 2022. Terrestrial ecosystem response to flash droughts over India. *Journal of*
466 *Hydrology*. 605: 127402.

- 467 Qing, Y., Wang, S., Ancell, B.C., Yang, Z., 2022. Accelerating flash droughts induced by the joint influence of soil moisture
468 depletion and atmospheric aridity. *Nat. Commun.* 13 (1).
- 469 Rigden, A. J., Mueller, N. D., Holbrook, N. M., Pillai, N., & Huybers, P. 2020. Combined influence of soil moisture and
470 atmospheric evaporative demand is important for accurately predicting US maize yields. *Nature Food*, 1(2), 127–133.
- 471 Ru J, Wan S, Hui D, et al., 2023. Overcompensation of ecosystem productivity following sustained extreme drought in a
472 semiarid grassland. *Ecology*. 104(4): e3997.
- 473 Sadiqi, S. S. J., Hong, E. M., Nam, W. H., & Kim, T. 2022. An integrated framework for understanding ecological drought
474 and drought resistance. *Science of The Total Environment*, 846, 157477.
- 475 Schwalm, C., Anderegg, W., Michalak, A. et al., 2017. Global patterns of drought recovery. *Nature*. 548, 202-205.
- 476 Sreeparvathy, V., Srinivas, V.V., 2022. Meteorological flash droughts risk projections based on CMIP6 climate change
477 scenarios. *npj Clim Atmos Sci* 5, 77.
- 478 Sun, H., Gui, D., Yan, B., et al., 2016. Assessing the potential of random forest method for estimating solar radiation using air
479 pollution index. *Energy Conversion and Management*. 119, 121-129.
- 480 Sun, H., Lu, M., Yang, Y., et al., 2023. Revisiting the role of transpiration in the variation of ecosystem water use efficiency
481 in China. *Agricultural and Forest Meteorology*, 332, 109344.
- 482 Tabari, H. & Willems, P., 2018. More prolonged droughts by the end of the century in the Middle East. *Environ. Res. Lett.* 13,
483 104005.
- 484 Tabari, H., Willems, P. 2023. Sustainable development substantially reduces the risk of future drought impacts. *Commun Earth*
485 *Environ* 4, 180.
- 486 Zotarelli, L., Dukes, M. D., Romero, C. C., et al., 2010. Step by step calculation of the Penman-Monteith Evapotranspiration
487 (FAO-56 Method). Institute of Food and Agricultural Sciences. University of Florida, 8.
- 488 Štrumbelj, E., & Kononenko, I., 2014. Explaining prediction models and individual predictions with feature contributions.
489 *Knowledge and information systems*, 41, 647-665.

490 Tuinenburg, O. A., Bosmans, J. H. C., Staal, A., 2022. The global potential of forest restoration for drought mitigation.
491 Environmental Research Letters. 17(3): 034045.

492 Tyagi, S., Zhang, X., Saraswat, D., et al., 2022. Flash Drought: Review of Concept, Prediction and the Potential for Machine
493 Learning, Deep Learning Methods. Earth's Future. 10(11): e2022EF002723.

494 Vicente-Serrano, S. M., Gouveia, C., Camarero, J. J., et al. 2013. Response of vegetation to drought time-scales across global
495 land biomes. Proceedings of the National Academy of Sciences of the United States of America, 110(1), 52-57.

496 Wang, L., Yuan, X., Xie, Z., et al., 2016. Increasing flash droughts over China during the recent global warming hiatus. Sci
497 Rep. 6:30571.

498 Wang, Y., & Yuan, X., 2022a. Land-atmosphere coupling speeds up flash drought onset. Science of The Total Environment,
499 851, 158109.

500 Wang, S., Peng, H., & Liang, S., 2022b. Prediction of estuarine water quality using interpretable machine learning approach.
501 Journal of Hydrology. 605, 127320.

502 Wang, H., Zhu, Q., Wang, Y., et al., 2023a. Spatio-temporal characteristics and driving factors of flash drought recovery: From
503 the perspective of soil moisture and GPP changes. Weather and Climate Extremes. 42: 100605.

504 Wang, Y., & Yuan, X. 2023b. High temperature accelerates onset speed of the 2022 unprecedented flash drought over the
505 Yangtze River Basin. Geophysical Research Letters, 50(22), e2023GL105375.

506 WMO. 2021. WMO Atlas of Mortality and Economic Losses from Weather, Climate and Water Extremes (1970–2019).
507 WMO-No. 1267.

508 Wu, X., Liu, H., Li, X., et al., 2017. Differentiating drought legacy effects on vegetation growth over the temperate Northern
509 Hemisphere. Global Change Biology. 24(1), 504-516.

510 Xi, X., Liang, M., & Yuan, X. 2024. Increased atmospheric water stress on gross primary productivity during flash droughts
511 over China from 1961 to 2022. Weather and Climate Extremes, 44, 100667.

512 Xu, S., Wang, Y., Liu, Y., et al., 2023. Evaluating the cumulative and time-lag effects of vegetation response to drought in
513 Central Asia under changing environments. Journal of Hydrology. 130455.

- 514 Yang, L., Wang, W., Wei, J., 2023. Assessing the response of vegetation photosynthesis to flash drought events based on a
515 new identification framework. *Agricultural and Forest Meteorology*. 339: 109545.
- 516 Yang, K., He, J., Tang, W., et al., 2019. China meteorological forcing dataset (1979-2018). A Big Earth Data Platform for
517 Three Poles. <https://doi.org/10.11888/AtmosphericPhysics.tpe.249369.file>.
- 518 Yang, L., Wang, W., Wei, J., 2023. Assessing the response of vegetation photosynthesis to flash drought events based on a
519 new identification framework. *Agricultural and Forest Meteorology*. 339: 109545.
- 520 Yang, Y. T., Guan, H. D., Batelaan, O., et al., 2016. Contrasting responses of water use efficiency to drought across global
521 terrestrial ecosystems. *Scientific Reports*, 6, 23284.
- 522 Yao, T., Liu, S., Hu, S, et al., 2022. Response of vegetation ecosystems to flash drought with solar-induced chlorophyll
523 fluorescence over the Hai River Basin, China during 2001–2019. *Journal of Environmental Management*. 313: 114947.
- 524 Yu, Z., Wang, J., Liu, S., et al., 2017. Global gross primary productivity and water use efficiency changes under drought stress.
525 *Environmental Research Letters*, 12(1), 014016.
- 526 Yuan, X., Wang, L., Wu, P., Ji, P., Sheffield, J., Zhang, M., 2019. Anthropogenic shift towards higher risk of flash drought
527 over China. *Nat. Commun.* 10 (1).
- 528 Zha, X., Xiong, L., Liu, C., Shu, P., & Xiong, B., 2023. Identification and evaluation of soil moisture flash drought by a
529 nonstationary framework considering climate and land cover changes. *Science of the Total Environment*, 856, 158953.
- 530 Zhang, X., Chen, N., Sheng, H., et al. 2019. Urban drought challenge to 2030 sustainable development goals. *Science of the*
531 *Total Environment*. 693: 133536.
- 532 Zhang, M., Yuan, X., 2020a. Rapid reduction in ecosystem productivity caused by flash droughts based on decade-long
533 FLUXNET observations. *Hydrology and Earth System Sciences*. 24(11): 5579-5593.
- 534 Zhang, M., Yuan, X., & Otkin, J. A., 2020b. Remote sensing of the impact of flash drought events on terrestrial carbon
535 dynamics over China. *Carbon Balance and Management*, 15(1), 1-11.
- 536 Zhang, S., Yang, Y., Wu, X., et al., 2021. Post drought recovery time across global terrestrial ecosystems. *Journal of*
537 *Geophysical Research: Biogeosciences*. 126(6): e2020JG005699.

- 538 Zhang, S., Li, M., Ma, Z., et al., 2023. The intensification of flash droughts across China from 1981 to 2021. *Clim Dyn.*
539 <https://doi.org/10.1007/s00382-023-06980-8>.
- 540 Zomer, R.J., Xu, J. & Trabucco, A., 2022. Version 3 of the Global Aridity Index and Potential Evapotranspiration Database.
541 *Sci Data* 9, 409.